ELSEVIER

Thermochimica Acta 378 (2001) 135–144

thermochimica acta

www.elsevier.com/locate/tca

Isothermal and non-isothermal crystallization kinetics of zinc-aluminosilicate glasses

E. Tkalcec*, S. Kurajica, H. Ivankovic

Faculty of Chemical Engineering and Technology, University of Zagreb, 19 Marulicev trg, HR-10000 Zagreb, Croatia

Received 20 February 2001; received in revised form 14 May 2001; accepted 5 June 2001

Abstract

Isothermal and non-isothermal differential thermal analysis (DTA), and X-ray diffraction (XRD) were used to study the nucleation and crystallization behavior of multicomponent Li_2O–ZnO–Al_2O_3–B_2O_3–SiO_2 glasses with ZrO_2 and TiO_2 as nucleating agents. The temperature of maximum nucleation rate for investigated glasses was found to be 1028 K. The crystallization of two phases (mullite s.s. and gahnite) occurs in a narrow temperature and time interval, respectively, therefore, the DTA curves are characterized by the superposition of exothermic peaks. Recently derived mathematical models have been applied for resolving the overlapping. The models enabled establishing the kinetic parameters for crystal growth of individual phases. The activation energies for crystal growth were found to be in the range of 459–471 and 368–386 kJ mol^{-1} for mullite and gahnite, respectively. Avrami exponent n reveals three-dimensional growth of both phases. © 2001 Elsevier Science B.V. All rights reserved.

Keywords: Crystallization kinetics; Differential thermal analysis; Gahnite; Glass–ceramics; Overlapping

1. Introduction

Transparent glass–ceramics derived from the zinc-aluminoslilicate glasses with mullite ($Al^{VI}[Al^{IV}_{2+2x}Si_{2-2x}O_{10-x}]$) and gahnite ($ZnAl_2O_4$) as the predominant crystalline phases has drawn attention because of its potential application as a host for luminescent ions [1–5]. In order to obtain a fine microstructure and transparency an intense nucleation effect is essential [6,7]. The parameters that should be known for glasses used for glass–ceramics applications include the temperature range of nucleation, the temperature of maximum nucleation rate and the crystallization kinetic parameters, which provide the possibility to determine the mechanisms of nucleation and crystal growth processes.

Different methods can be used for estimating the kinetic parameters of glass crystallization. Differential thermal analysis (DTA) is of particular importance in such studies, and the techniques can be broadly classified into isothermal and non-isothermal methods. Numerous treatments for the determination of the kinetic parameters in non-isothermal [8–13], and isothermal [14–18] conditions have been described. In the case of superimposed DTA effects, however, these treatments are inapplicable [19].

In this work, the crystallization of Li_2O–ZnO–Al_2O_3–B_2O_3–SiO_2 glass in the presence of ZrO_2 and TiO_2 as nucleating agents with the molar ratios of $ZrO_2/TiO_2 = 2/3$ and 3/2 were studied. The crystallization kinetics have been studied in non-isothermal

* Corresponding author. Fax: +385-1-4597-250.
E-mail address: etkalcec@pierre.fkit.hr (E. Tkalcec).

0040-6031/01/$ – see front matter
PII: S0040-6031(01)00627-X

and isothermal conditions using DTA. Recently developed mathematical models for non-isothermal [20] and isothermal kinetic analysis [21] of overlapped DTA peaks occurring due to simultaneous crystallization processes have been used.

2. Experimental procedure

2.1. Glass preparation

The batch compositions of investigated glasses are given in Table 1. The sum of nucleation agents (ZrO_2 and TiO_2) is constant in both glasses, whereas the molar ratio of ZrO_2/TiO_2 varies. It is 2/3 and 3/2 in glass Z2T3 and Z3T2, respectively. The mixture of quartz sand (Sibelco, chemical analysis in wt.%: 99.75 SiO_2, 0.055 Al_2O_3, 0.010 Fe_2O_3, 0.020 TiO_2, 0.005 K_2O, 0.005 CaO, loss on ignition 0.08) and reagent grade chemicals of $Al(OH)_3$, H_3BO_3, ZnO, TiO_2, ZrO_2 and Li_2O were melted in Pt crucible in electrical furnace for 2 h at 1873 ± 5 K. The impurities in quartz sand were taken into consideration by batch composition). Glasses were crushed and remelted for another 2 h at the same temperature. Remelted melts were poured onto a heated steel plate to form a round disc about 5 mm thick, then transferred into a heated furnace at 873 K for annealing, and cooled down in the furnace 12 h.

2.2. Methods and analyses

DTA was performed using thermoanalyser Netzsch STA 409 under a constant synthetic air flow of 30 $cm^3\ min^{-1}$. Pt crucibles, and alumina as a reference were used. DTA analysis was carried out on powdered and nucleated glass samples with particle size <63 μm. To define the temperature of maximum nucleation rate, T_{mn}, DTA runs were carried out as follows: during each DTA run, a glass sample was heated at a rate of 20 K min^{-1} to temperature T_n in the temperature range between 993 and 1073 K, nucleated at chosen temperature for 2 h and subsequently heated to 1373 K at the rate of 10 K min^{-1}, without being removed from DTA apparatus. Various nucleation temperatures, T_n, exhibited different peak temperatures on DTA scans, T_p. According to Ray and Day [22], the plot of peak temperatures, T_p, versus the temperature of nucleation, T_n, displays minimum, which represents the temperature of maximum nucleation rate, T_{mn}.

For determination of crystallization kinetics under non-isothermal conditions, glass samples were first heated to the previously determined T_{mn} at the heating

Table 1
Batch compositions and sample notations

Sample notations	Composition (mol%)						
	SiO_2	Al_2O_3	B_2O_3	ZnO	Li_2O	TiO_2	ZrO_2
Z2T3	62.6	18.6	3.9	9.3	1.7	1.5	2.3
Z3T2	62.6	18.6	3.9	9.3	1.7	2.3	1.5

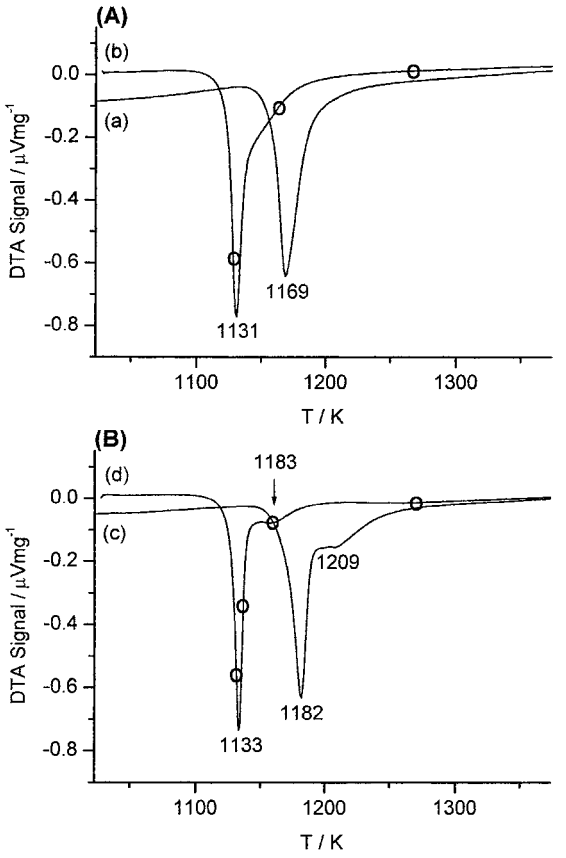

Fig. 1. DTA scans of glasses at the heating rate of 10 K min^{-1}: (A) Z2T3 glass, (a) as-quenched, (b) nucleated at 755 °C for 2 h; (B) Z3T2 glass, (c) as-quenched, (d) nucleated. (○) The temperatures at which the scans were interrupted and the samples submitted to XRD analyses.

rate of 20 K min^{-1} nucleated at this temperature for 2 h, and then further heated at the rates of 2.5, 5, 10, 15 and 20 K min^{-1} to 1373 K.

The isothermal experiments were carried out by heating the samples to the previously determined temperature of maximum nucleation rate, T_{mn}, at the heating rate of 20 K min^{-1}, nucleated at this temperature for 2 h, and then heated to a desired annealing temperature at the heating rate of 20 K min^{-1}. The annealing temperatures were selected in the ranges between 1061 and 1095 K (glass Z2T3) or between 1067 and 1100 K (glass Z3T2) because the glasses show reasonable peak intensities for data analysis in these ranges. The samples were held on attained temperatures until the end of the crystallization process.

The phase analysis of glasses crystallized during DTA runs was carried out by X-ray diffraction (XRD). To establish the path of crystallization, heating in DTA apparatus was interrupted in the vicinity of some characteristic DTA scan points (peak maximum, or inflection point, etc.) and the samples were fast cooled down to room temperature and then submitted to XRD.

3. Results

3.1. Non-isothermal kinetics

DTA scans of as-quenched glasses Z2T3 and Z3T2 at a heating rate of 10 K min^{-1} are shown in Fig. 1. Glass Z2T3 (Fig. 1A) exhibits one exothermic peak with the maximum at $T_p = 1169$ K. By nucleation, the peak is shifted toward lower temperature ($T_p = 1131$ K) and becomes slightly asymmetrical. The glass Z3T2 (Fig. 1B), however, exhibits two overlapping

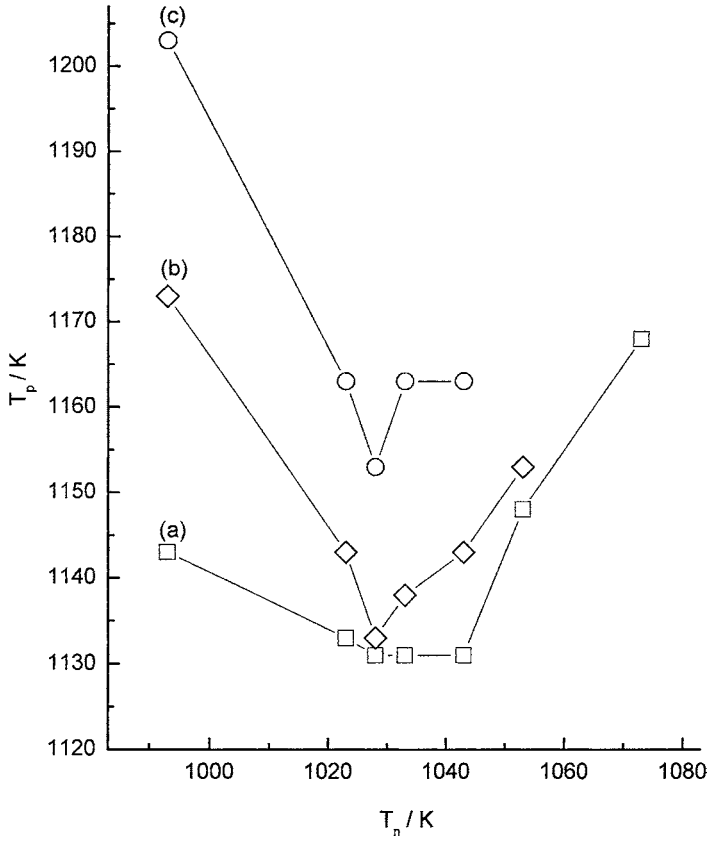

Fig. 2. DTA peak temperature, T_p, vs. nucleation temperature, T_n: (a) glass Z2T3; (b) first peak of glass Z3T2; (c) second peak of glass Z3T2. The lines are drawn as a guide for the eye.

exothermic peaks; a sharp one at $T_{p1} = 1182$ K and smaller one at about $T_{p2} = 1210$ K. Two overlapping peaks are observed for the nucleated glass too. By nucleation the both peaks are shifted toward lower temperatures; from 1182 to 1134 and 1210 to 1163 K, respectively.

Ray and Day [22] pointed out that the increase of nuclei in a glass causes a decrease in DTA peak temperature, T_p, and it reaches a minimum if a glass was heat treated at the temperature at which a maximum number of nuclei were formed. To determine the temperature of maximum nucleation rate, T_{mn}, the authors [22] used the plot of DTA peak temperature, T_p, versus the temperature of the nucleation, T_n. The minimum on such plot represents the temperature of maximum nucleation rate, T_{mn}. Following the suggested method, we have constructed the plots of T_p versus T_n for both glasses, which are given in Fig. 2. For glass Z3T2, this plot yields a minimum at 1028 K (plot 'b' for the first peak and plot 'c' for the second DTA peak). The same plot for glass Z2T3 shows no minimum but exhibits a plateau in the range from 1028 to 1043 K (Fig. 2, plot 'a'). Since in the glass Z2T3 nucleated at 1028 K, no crystalline phase on XRD pattern was observed, 1028 K was selected as the temperature of nucleation for Z2T3 glass too. The phases crystallizing during DTA runs were ascertained by interrupting DTA scans at the temperatures marked in Fig. 1 and by submitting the quenched samples to XRD analysis. Fig. 3 shows XRD patterns of the glass Z2T3 quenched from the marked temperatures. At 1129 K, mullite s.s. and small amount of gahnite were observed. With increasing temperature, increases the amount of gahnite and at 1161 K starts to crystallize one of the nucleating agents ZrO_2. The phases are correlated with the corresponding JCPDS data, which are also presented in the figure. The same path of crystallization was observed in the glass Z3T2, only a greater amount of cubic-ZrO_2 was observed.

The sets of non-isothermal DTA scans of previously nucleated samples heated at the rates of 2.5, 5, 10, 15 and 20 K min^{-1} are shown in Fig. 4. Although the separation of exothermic peaks is enhanced by nucleation, the degree of overlapping is still great, especially

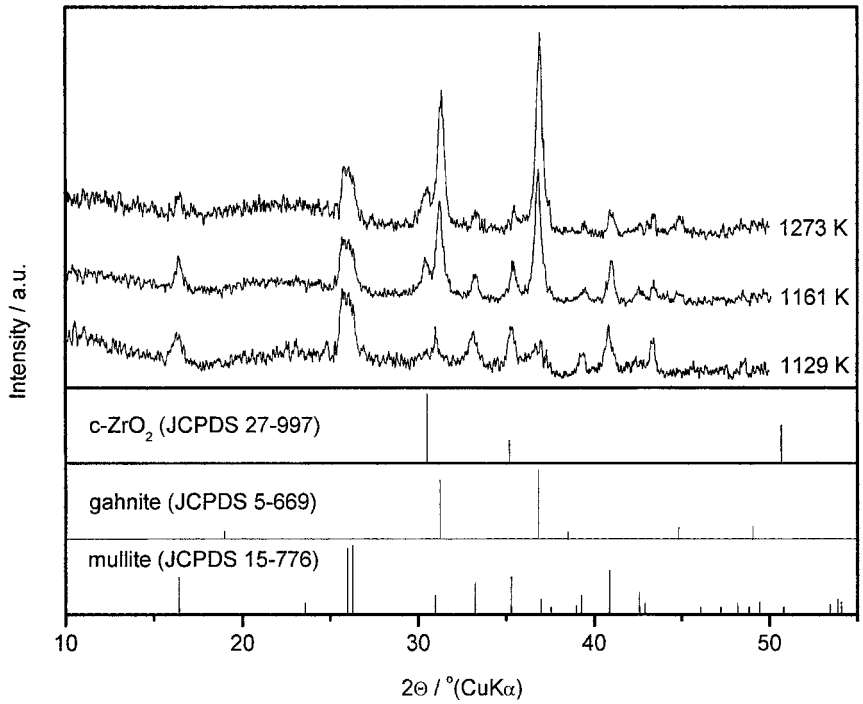

Fig. 3. XRD patterns of glass Z2T3 nucleated at 1028 K for 2 h and subsequently heated in DTA up to the temperatures given in the picture.

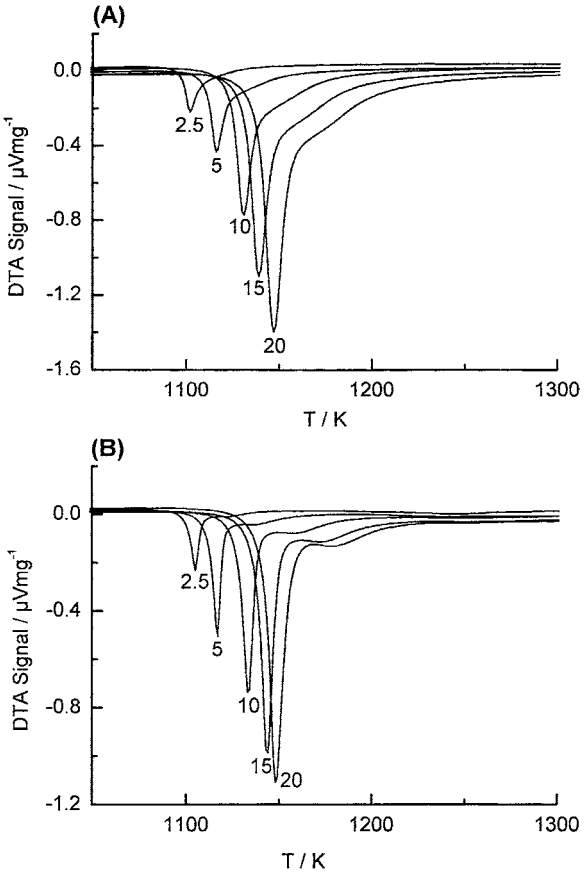

Fig. 4. DTA scans of the nucleated glasses heated at the rates of 2.5, 5, 10, 15 and 20 K min^{-1}: (A) glass Z2T3 and (B) glass Z3T2.

in glass Z2T3. Hence, the T_p values for the second phase could be only estimated, and the activation energy for crystallization of the second phase evaluated by Kissinger plot $\ln(\beta/T_p^2)$ versus $1/T_p$ [9] would be erroneous. Therefore, computer program for separating individual peaks, based on Eq. (1) [20], was applied.

$$\frac{d\alpha}{dT} = \sum_{i=1}^{2} w_i \left\{ \left[-a_i \exp\left(\frac{a_i}{T}\right) + b_i \right] \times \left[\frac{\exp[-\exp((a_i/T) + b_i)]}{T^2} \right] \right\} \quad (1)$$

where w_i is the ratio between the first (or the second) resolved peak area and the total peak area, $a_i = -(n_i E_i/R)$, n_i the Avrami exponent, E_i the activation energy for crystallization, R the gas constant, $b_i = \ln(k_i^n/\beta^n)$, k_i the rate constant and β the linear heating rate. The overlapping DTA peaks shown in Fig. 4 are resolved successfully, and satisfactory matching of experimental and calculated curves was obtained. The match of fit to experimental DTA scan for glass Z2T3 at the heating rate of 2.5 K min^{-1} is shown as an example in Fig. 5. Table 2 summarizes the calculated temperatures at various heating rates. The values read directly on DTA scans are given in brackets. Activation energies evaluated, applying Kissinger method [9], are given in Table 4.

3.2. Isothermal kinetics

Isothermal measurements were performed to test the validity of the results obtained under non-isothermal conditions and to determine Avrami exponent n for both phases. The isothermal DTA scans are shown in Fig. 6. It is worth to note that if there is an overlapping of two DTA peaks in non-isothermal experiment, the degree of overlapping in an isothermal experiment is expected to be much larger [23].

Table 2
Calculated DTA peak temperatures, T_{p1} and T_{p2} (Eq. (1))[a]

Heating rate, β (K min^{-1})	Nucleated glass Z2T3 (K)		Nucleated glass Z3T2 (K)	
	T_{p1}	T_{p2}	T_{p1}	T_{p2}
2.5	1102.9 (1101)	1112.8 (n.d.)[b]	1105.1 (1105)	1112.8 (1123)
5	1117.1 (1116)	1130.6 (n.d.)	1116.8 (1117)	1130.6 (1139)
10	1131.7 (1131)	1148.9 (n.d.)	1133.7 (1133)	1148.9 (1160)
15	1140.1 (1139)	1159.7 (n.d.)	1144.1 (1144)	1159.7 (1176)
20	1148.2 (1147)	1170.5 (n.d.)	1149.3 (1148)	1170.5 (1183)

[a] The values read directly on DTA scans are given in brackets.
[b] n.d.: Not determinable.

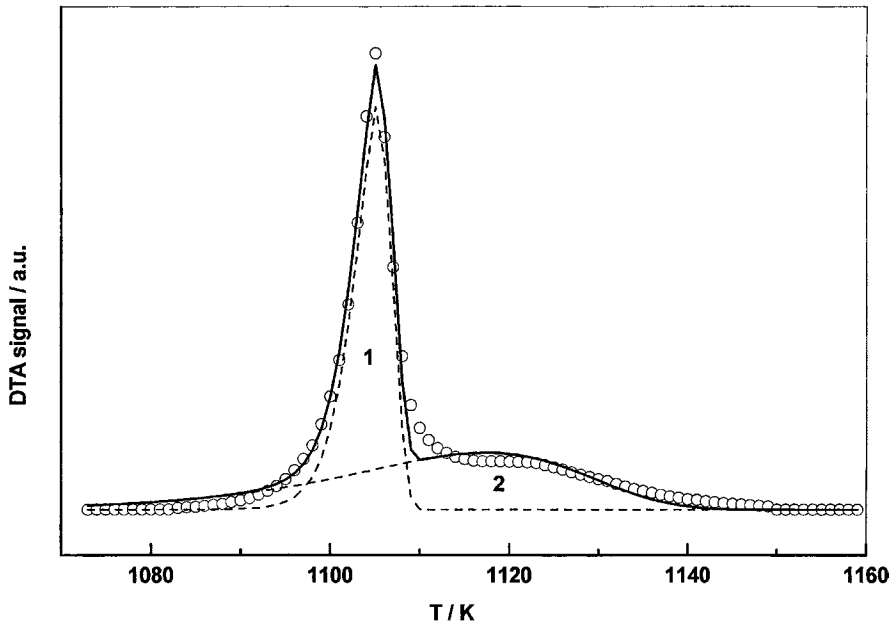

Fig. 5. Fit of DTA scan for Z3T2 at the heating rate of 2.5 K min^{-1}: (○) experimental DATA; (1) peak attributed to mullite s.s.; (2) peak attributed to gahnite. The solid line is a fit to experimental data.

Interrupting the isothermal DTA runs at different time points and subjecting the obtained specimen to XRD, it was confirmed that in fact the same two different phases as in non-isothermal experiment (mullite s.s. and gahnite) crystallize during one exothermic peak.

In the case of one-phase crystallization process, the volume fraction transformed as a function of time, $\alpha(t)$, could be fitted to the Johnson–Mehl–Avrami (JMA) kinetic model [14–17]. However, this model is useless if two phases crystallize in the same time interval. Therefore, we fitted the experimental DTA scans to two-phase model recently reported by us [21], which is defined by Eq. (2).

$$\frac{d\alpha}{dt} = w_i \sum_{i=1}^{2} \{[k_i^{n_i} n_i (t-\tau_i)^{(n_i-1)}] \exp[-k_i^{n_i}(t-\tau)^{n_i}]\} \quad (2)$$

Table 3
Calculated kinetic parameters k_1, n_1 k_2, and n_2 obtained applying two-phase model for glass crystallization under isothermal conditions (Eq. (2))

Glass Z2T3					Glass Z3T2				
T (K)	k_1[a] (min^{-1})	k_2[a] (min^{-1})	n_1	n_2	T (K)	k_1 (min^{-1})	k_2 (min^{-1})	n_1	n_2
1061	0.031 (1)	0.117 (7)	3.06 (2)	3.39 (2)	1067	0.030 (4)	0.096 (2)	3.75 (2)	2.92 (8)
1066	0.042 (1)	0.147 (4)	3.15 (1)	3.37 (1)	1072	0.034 (1)	0.122 (2)	4.08 (1)	2.84 (7)
1070	0.043 (1)	0.173 (4)	3.23 (2)	3.15 (2)	1076	0.047 (1)	0.131 (2)	3.20 (2)	2.94 (9)
1076	0.052 (1)	0.201 (6)	3.11 (2)	3.04 (2)	1081	0.056 (1)	0.152 (2)	3.20 (1)	3.09 (7)
1081	0.067 (1)	0.273 (4)	3.24 (2)	3.16 (2)	1087	0.078 (1)	0.206 (3)	3.14 (1)	3.25 (9)
1085	0.088 (1)	0.345 (5)	3.13 (2)	3.12 (2)	1090	0.085 (1)	0.236 (3)	3.44 (1)	3.31 (8)
1090	0.122 (1)	0.379 (4)	2.81 (2)	3.32 (2)	1095	0.110 (1)	0.270 (3)	3.04 (1)	3.44 (9)
1095	0.162 (1)	0.424 (2)	3.38 (2)	3.16 (2)	1100	0.141 (2)	0.346 (3)	3.06 (1)	3.50 (9)

[a] Subscript 1: mullite s.s.; subscript 2: gahnite.

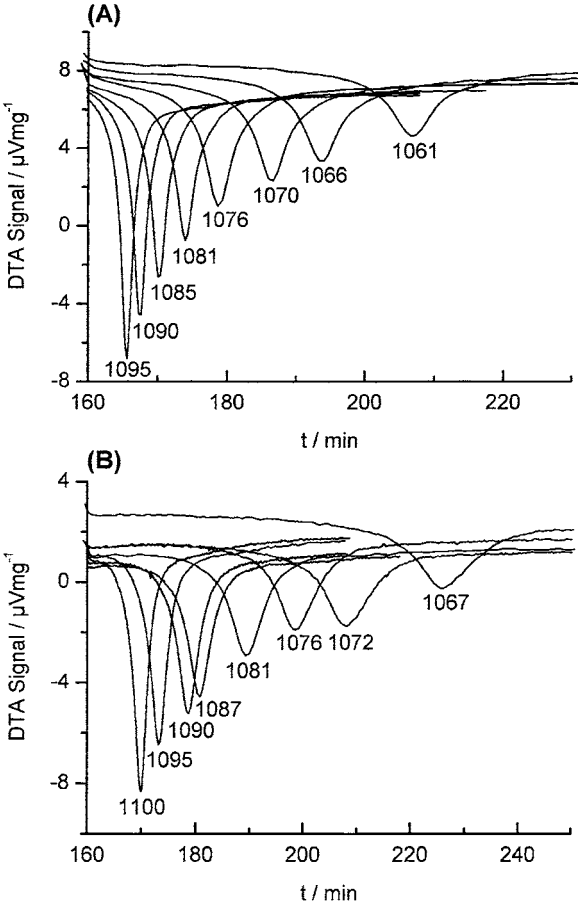

Fig. 6. Isothermal DTA scans of glasses nucleated at 1028 K for 2 h: (A) glass Z2T3 and (B) glass Z3T2. The annealing temperatures (K) are given in the figure.

where w_i is the ratio between the first (or the second) resolved peak area and the total peak area on DTA scan, n_i the Avrami exponent, k_i the rate constant, and τ_i a term which accounts for incubation time.

The observed DTA scans in Fig. 6 have been resolved into separated peaks and Eq. (2) fits rather good the experimental DTA. Fig. 7 shows the DTA scan and the fit for sample Z2T3 annealed at 1073 K. Table 3 summarizes the corresponding results obtained for nucleated glasses annealed at various temperatures. Rate constants k_1 and k_2 are assumed to follow Arrhenius dependence: $k = k_0 \exp(-E/RT)$, where E is the activation energy for crystallization. From the slope of the Arrhenius plots, the activation energies for crystallization of each of the individual phases, i.e. for mullite s.s. (E_m) and gahnite (E_g) under isothermal conditions are derived. The values obtained are: $E_m = 459 \pm 33$ kJ mol^{-1} and $E_g = 386 \pm 19$ kJ mol^{-1} for Z2T3 glass, and $E_m = 461 \pm 18$ kJ mol^{-1} and $E_g = 370 \pm 14$ kJ mol^{-1} for Z3T2 glass, respectively.

4. Discussion

4.1. Non-isothermal conditions

DTA scan of non-nucleated glass Z2T3 ($ZrO_2/TiO_2 = 2/3$) (Fig. 1A) exhibits one exothermic peak with the maximum at $T_p = 1169$ K which suggests the conclusion that only one crystalline phase occurs. This is, however, in contradiction with XRD analysis. By nucleation at 1028 K, the peak becomes slightly asymmetrical. That implies rather two overlapping processes than single one in the same temperature range, which is in accordance with XRD (Fig. 3). For the glass Z3T2 ($ZrO_2/TiO_2 = 3/2$) (Fig. 1B), these two crystallizing processes are better resolved and the crystallization occur at higher temperatures. By nucleation of the glasses at 1028 K for 2 h, a shift to lower temperature and better resolution of crystallization were observed. Following the method suggested by Ray and Day [22], the temperature of maximum nucleation rate T_{mn} was found to be 1028 K for both DTA peaks. However, for the glass Z2T3 only a plateau between 1028 and 1043 K is obtained, which is attributed to the folding over the nucleation and crystallization [24], and is already reported for zinc-aluminosilicate glasses [25]. It was recommended [24] to take the highest temperature at which T_p yields the same constant value (i.e. the end of the plateau) as the temperature of maximum nucleation rate, T_{mn}. However, it seems to us more reasonable to use the lowest temperature of plateau to avoid the crystallization. Therefore, 1028 K was selected as the temperature of maximum nucleation rate for Z2T3 glass too. It is in a good agreement with the value obtained by Strnad [26], who used the microscopic method to determine the temperature of maximum nucleation rate in gahnite glass–ceramics. Glass Z2T3 nucleated at 1028 K for 2 h exhibited no crystalline phase on XRD pattern.

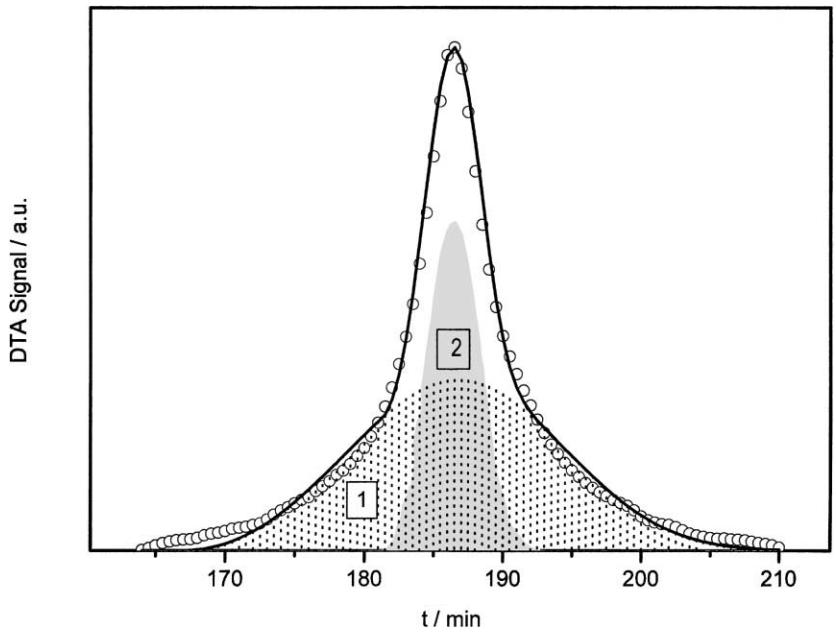

Fig. 7. Isothermal DTA scan of glass Z2T3 at 1073 K: (○) experimental data; (1) separated mullite exotherm; (2) separated gahnite exotherm. Solid line is the best-fit of Eq. (2) to experimental data.

Although the separation of exothermic peaks is enhanced by nucleation, the degree of overlapping is still great (Fig. 4). It is especially large in glass Z2T3, and the second DTA peak T_{p2} is not determinable (Table 2). Therefore, the overlapping peaks were resolved using the method described by us previously [20]. The peaks were resolved successfully, and satisfactory matching of experimental and calculated curves was obtained (Fig. 5). In such manner, the T_{p2} values for the glass Z2T3, previously undeterminable, became determinable, and more reliable T_{p2} values for Z3T2 were attained. The calculated T_{p1} values are almost the same as read directly from DTA scans for both glasses. XRD analyses of nucleated glasses (Fig. 3) reveal that the first DTA peak can be attributed to crystallization of mullite solid solution ($Al^{VI}[Al^{IV}_{2+2x}Si_{2-2x}O_{10-x}]$), while the second peak to gahnite ($ZnAl_2O_4$). It has to be noticed that there is no temperature range in which mullite s.s. or gahnite crystallizes as the sole phase. Cubic-zirconium oxide (c-ZrO_2) is determined in the glass Z2T3 ($ZrO_2/TiO_2 = 2/3$) at 1161 K, and in the glass Z3T2 ($ZrO_2/TiO_2 = 3/2$) at 1123 K (heating rate of DTA runs 10 K min^{-1}). Since the glasses were nucleated, it can be assumed that the activation energies evaluated from the Kissinger method [9] are only due to crystal growth [27] of mullite s.s. and gahnite, respectively. The obtained values are: for mullite s.s. $E_m = 471 \pm 10$ kJ mol^{-1} and for gahnite $E_g = 377 \pm 10$ kJ mol^{-1} for Z2T3 glass, and $E_m = 461 \pm 19$ kJ mol^{-1} and $E_g = 368 \pm 15$ kJ mol^{-1} for Z3T2 glass. The difference between the values for the same phase in two different glasses are within the calculation error span, therefore it is reasonable to assume that there is no influence of the nucleation agent ratios on kinetic parameters of mullite s.s. and gahnite.

4.2. Isothermal conditions

Since two phases (mullite s.s. and gahnite) crystallize at any annealing temperature exhibiting single exothermic peak as shown in Fig. 6, it was not reasonable to fit the crystallization peak by any single JMA kinetics. Hence, the experimental data were fitted to two-phase model (Eq. (2)). The satisfactory matching of experimental and calculated curves (Fig. 7) shows that the use of two-phase model is appropriate and reveals that mullite s.s. starts to crystallize first, whereas gahnite begins to crystallize with a small

Table 4
Activation energies for crystal growth of mullite s.s. and gahnite (kJ mol^{-1}) obtained using Kissinger plot (non-isothermal conditions) and Arrhenius plot (isothermal conditions)

	Glass Z2T3		Glass Z3T2	
Experimental conditions	Non-isothermal	Isothermal	Non-isothermal	Isothermal
Mullite	471 ± 10	459 ± 33	461 ± 19	461 ± 18
Gahnite	377 ± 10	386 ± 19	368 ± 15	370 ± 14

time lag. Moreover, it was possible to determine the time window in which the crystallization of gahnite proceeds (Fig. 7). It yields only ca. 10 min at 1073 K, and is completely overlapped by mullite crystallization, which is extended over larger time range. As shown in Table 3, the rate of mullite crystallization is smaller than of gahnite, and three-dimensional growth for both phases could be assumed. The activation energies obtained in non-isothermal and those obtained in isothermal conditions (Table 4) were the same within experimental error. The obtained activation energy for gahnite agrees with the value for crystal growth cited by Šestak [28] from optical measurements (314 kJ mol^{-1}). This fact could confirm the assumption that the evaluated activation energies are due to crystal growth. The fit of Eq. (2) provides a very good description in the middle part of the measurement, while there is a less good description around the initial time and at the end of DTA scan. Different reasons could be encountered as the cause of these deviations. Systematic errors may arise due to possible effects such as initial reactions which cannot be avoided during heat-up, wrong determined incubation time, τ, wrong determined base line, not sufficient time of nucleation, etc. [29].

5. Conclusions

The crystallization kinetics of multicomponent Li_2O–ZnO–Al_2O_3–B_2O_3–SiO_2 glasses with different ZrO_2/TiO_2 ratios has been studied in non-isothermal and isothermal conditions using DTA. Under non-isothermal conditions, mullite s.s. is the predominant phase at lower temperature and gahnite at higher temperature. Under isothermal conditions, the time window of gahnite crystallization is very narrow (about 10 min at 1273 K), whereas mullite crystallizes in broader time range. Recently proposed models (Eqs. (1) and (2)) for resolution of overlapping peaks can be satisfactorily applied. The activation energies of crystal growth for mullite s.s. and gahnite were found to be independent on the ratio of ZrO_2/TiO_2 and on experimental conditions.

The temperature of maximum nucleation rate ($T_n = 1028$ K) determined by the shift of the DTA peak, T_p, with the nucleation temperature, T_n, is in a good agreement with the value obtained by the more time-consuming classical microscopic technique.

The calculated values of activation energies for growth of mullite s.s. were 459–471 kJ mol^{-1} and for gahnite 368–386 kJ mol^{-1}. Avrami exponent n reveals three-dimensional growth of both phases.

Acknowledgements

This material is based on work supported by the Ministry of Science and Technology of the Republic of Croatia. The authors would like to thank Dr. A. Bezjak for valuable comments and discussions concerning this work.

References

[1] P.D. Sarkisov, in: O.V. Mazurin (Ed.), Survey Papers of the 15th International Congress on Glass, Nauka, Leningrad, 1989, p. 441.
[2] G.H. Beall, J. Non-Cryst. Solids 73 (1985) 413.
[3] R. Reisfeld, Mater. Sci. Eng. 71 (1985) 375.
[4] R. Reisfeld, A. Kisilev, E. Greenberg, A. Buch, M. Ish-Shalom, Chem. Phys. Lett. 104 (1984) 153.
[5] C. Wang, W. Xu, J. Non-Cryst. Solids 80 (1986) 237.
[6] M. Tashiro, J. Non-Cryst. Solids 73 (1985) 575.
[7] V. Maier, G. Muller, J. Am. Ceram. Soc. 70 (1987) 176.
[8] T. Kemeny, J. Šestak, Thermochim. Acta 110 (1987) 113.
[9] H.E. Kissinger, J. Res. Natl. Bur. Stand. (U.S.) 57 (1956) 217.

[10] T. Ozawa, J. Therm. Anal. 2 (1970) 301.
[11] J.A. Augius, J.E. Bennet, J. Therm. Anal. 13 (1978) 283.
[12] K. Matusita, T. Komatsu, R. Yokota, J. Mater. Sci. 19 (1984) 219.
[13] X.J. Xu, C.H.S. Ray, D.E. Day, J. Am. Ceram. Soc. 74 (1991) 160.
[14] W.A. Johnson, R.F. Mehl, Trans. Am. Inst. Min. Metall. Pet. Eng. 135 (1939) 416.
[15] M. Avrami, J. Chem. Phys. 7 (1939) 1103.
[16] M. Avrami, J. Chem. Phys. 8 (1940) 212.
[17] M. Avrami, J. Chem. Phys. 9 (1941) 177.
[18] C.V. Thompson, A.L. Greer, F. Spaepen, Acta Metall. 31 (1983) 1883.
[19] A. Bezjak, E. Tkalčec, H. Ivanković, M. Ereš, Thermochim. Acta 221 (1993) 23.
[20] S. Kurajica, A. Bezjak, E. Tkalčec, Thermochim. Acta 288 (1996) 123.
[21] S. Kurajica, A. Bezjak, E. Tkalcec, Thermochim. Acta 360 (2000) 63.
[22] C.S. Ray, D.E. Day, J. Am. Ceram. Soc. 73 (1990) 439.
[23] E.J. Mittemeijer, J. Mater. Sci. 27 (1992) 3977.
[24] S. Gleditzsch, P. Helmold, Silikattechnik 40 (1989) 46.
[25] E. Tkalčec, H. Ivanković, S. Kurajica, Bol. Soc. Esp. Ceram. Vid. 31-C (1992) 5.
[26] Z. Strnad, Glass–ceramics Materials, Elsevier, Amsterdam, 1986, p. 148.
[27] K.F. Kelton, K. Lakashimi Narayan, L.E. Levine, T.C. Cull, C.S. Ray, J. Non-Cryst. Solids 204 (1996) 13.
[28] J. Šestak, Thermochim. Acta 280/281 (1996) 175.
[29] C. Michaelsen, M. Dahms, Thermochim. Acta 288 (1996) 9.